

Research Paper

Performance of geosynthetic reinforcement on the ballasted railway track

L.S. Sowmiya¹, J.T. Shahu², and K.K. Gupta³

ARTICLE INFORMATION

Article history:

Received: 04 March, 2015

Received in revised form: 26 June, 2015

Accepted: 06 July, 2015

Published on: September, 2015

Keywords:

Railway track

Ballast

Subballast

Subgrade

Geosynthetics

Model test

ABSTRACT

Geosynthetics provide an important option to improve track support stabilization and thereby reduce the track maintenance costs and operation costs due to train delays. In railroad construction, geosynthetics may be installed within or beneath the ballast or subballast layers. In this present study, model tests were performed on model tracks laid at 1:3 scale to the prototype with adequate thickness of subballast layer and placed on soft subgrade soils. Model tracks were adequately instrumented to record induced stresses and displacements in the track. Model tracks were reinforced with geogrid or geotextile or both at suitable interfaces. Track condition after a heavy rainfall was simulated. In this present study, three dimensional finite element analyses of geosynthetic reinforced railway track sections have been carried out using MIDAS/GTS 2013 and compared with unreinforced sections. The result shows that the reinforcement can be used to improve the performance of railway tracks on clayey subgrade.

1. Introduction

Railways form an important part of the transportation infrastructure of a country and plays an important role in sustaining a healthy economy. Indian Railways have now geared up to overhaul and upgrade its infrastructure to meet future demand of growing traffic. Indian railways have identified track-foundation-soil system as one of the key factors in bringing about these changes. Use of geosynthetics in civil engineering has advanced rapidly in recent years and it is now an internationally accepted material for various applications. Geotechnical aspects of design and construction of this infrastructure have a major influence on performance and maintenance cost (Raymond and Davies, 1978; Selig, 1991; Shahu et al., 1999). A literature review of model tests on unreinforced tracks show that in past, two types of tests, namely,

single sleeper tests (ORE, 1982) and full panel tests (ORE, 1983) have been performed on railway track models. Full panel tests are considered more accurate representation of the prototype owing to an accurate load transfer mechanism in such tests; these tests are also difficult to simulate and perform, and in general, requires large areal extent and handling of large quantity of material. Presently, few model test studies on reinforced tracks that are readily available in literature are single sleeper tests (Raymond, 2002; Shin et al., 2002; Indraratna et al., 2006; Brown, 2007). A majority of these studies except for Shin et al. (2002) were performed to investigate a reduction in ballast degradation in the presence of geogrid and as such, the focus of these studies was the behavior of the ballast layer and not the subgrade soil or the performance of the whole track. In fact, a thin rubber mat was used to simulate the subgrade

¹ Assistant Professor, Department of Civil Engineering, Indian School of Mines, Dhanbad-826004, INDIA, sowmiya_iitd@hotmail.com

² Professor & IALT member, Department of Civil Engineering, IIT Delhi, New Delhi-110016, INDIA, shahu@civil.iitd.ac.in

³ Retired Associate Professor, Department of Civil Engineering, IIT Delhi, New Delhi-110016, INDIA, kaushaliitd@hotmail.com

Note: Discussion on this paper is open until December 2015

instead of actual soil. Subgrade soil is a major component of the track foundation, and the subgrade settlement under traffic loading is known to be of the same order of magnitude as the combined settlement of the ballast and subballast layers (Sowmiya, 2013). The objective of the study is to examine the behavior of the geosynthetic reinforced railway tracks laid on soft subgrade soils. Accordingly, in this study, tests are performed on geosynthetic reinforced track models laid at 1:3 scale to the prototype with adequate thickness of subballast layer and placed on soft subgrade soil. Also, three dimensional finite element analyses of geosynthetic reinforced railway track sections have been carried out using MIDAS/GTS 2013 and compared with unreinforced sections.

2. Experimental program

An experimental study on the load-deformation behavior of different track constituent layers is conducted. A brief summary of the experimental program is given in Table 1.

The present study investigates the benefits of the use of geosynthetics on tracks laid on fine grained soils after a heavy monsoon rain in terms of track reinforcement. Monotonic and cyclic load tests are performed on model reinforced tracks with a subballast layer laid on compacted clayey subgrade. Track conditions after a heavy monsoon rain are simulated. The influence of subballast layer thickness and subgrade type on a load-deformation behavior of reinforced tracks under monotonic and cyclic loadings is evaluated.

3. Materials

Tests are performed on model tracks laid at 1:3 scale to the prototype. The materials used in the model tracks are described below. Grain size distributions of different model track materials are given in Fig.1 and typical characteristics are listed in Table 2. Photographs of these materials are shown in Figs. 2(a)-(e).

3.1 Ballast and subballast materials

Ballast is the selected crushed granular material placed as the top layer of the substructure in which the sleepers are embedded. The ballast was procured from an aggregate crushing plant at Manesar in Haryana state which also supplies ballast to Indian Railways (Fig. 2a). Subballast layer usually consists of a locally available free draining material (Shahu et al., 2000); therefore,

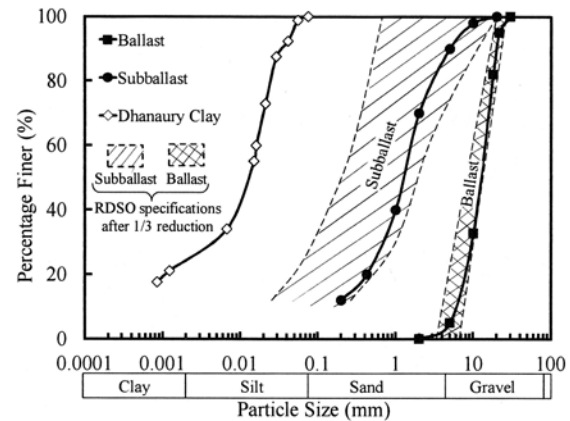


Fig. 1. Grain size distribution of various materials used in model tracks.

Table 1. Summary of tests conducted.

Layer and Material	Test Type
Ballast	Monotonic Triaxial (*CD Test)
Subballast	Monotonic Triaxial (CD Test)
Subgrade	Monotonic Triaxial (*CU Test)
Interface materials	Direct Shear test
Track	Monotonic and Cyclic test on model track

Note: *CD = Consolidated drained triaxial test

CU = Consolidated undrained triaxial test with pore water pressure measurement

Table 2. Summary of tests conducted.

Item	Ballast	Subballast	Dhanaury Clay
Classification	GW	SW	CI
$\gamma_{d(max)}$ (kN/m ³)	16.4	16.0	17.9
$\gamma_{d(min)}$ (kN/m ³)	14.2	11.7	-
OMC (%)	-	-	16.7
w _L (%)	-	-	36
I _p	-	-	15
k (m/s)	-	-	3.28x10 ⁻¹⁰

quarry dust from the same plant was used as the subballast material (Fig. 2b). Grain size distributions of the model ballast and subballast materials along with the range of prototype ballast and subballast materials specified by RDSO (Research Designs and Standards Organization, Indian Railways) after their one-third size reduction are given in Fig. 1.

3.2 Subgrade soil

Natural fine-grained soil, Dhanaury clay (DC) (Fig. 2e) is used as subgrade soils. In the present study, the subgrade condition after a heavy monsoon rain is simulated and hence laboratory tests are performed on remolded specimens of subgrade soils. Dhanaury clay

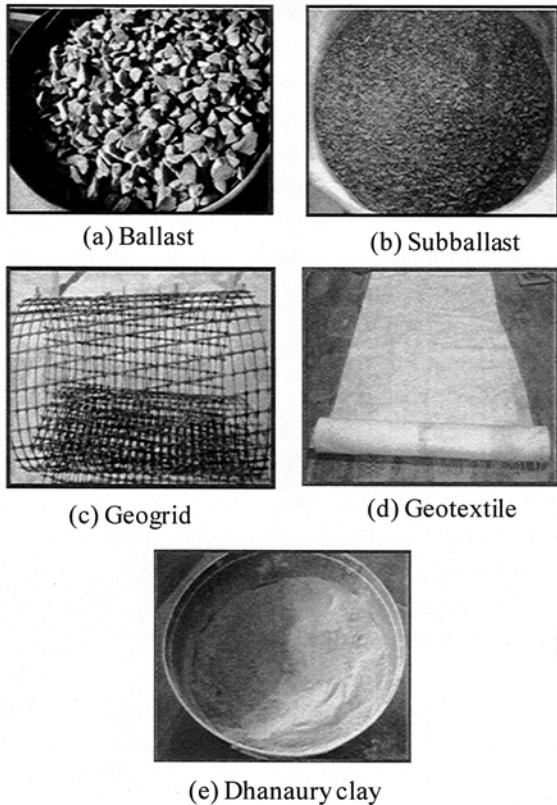


Fig. 2. Model track materials.

Table 3. Index properties of geosynthetic materials used for reinforcement.

Geosynthetic type	Geogrid	Geotextile
Polymer type	HDPE, Polyethylene	Polypropylene
Manufacturing type	Biaxial	Nonwoven, heat-bonded
Aperture size (mm)	MD = 30 mm; CD = 30 mm	-
Mass per unit area (g/m ²)	540 ^a	600 ^a
Thickness (mm)	2	2.2
Ultimate tensile strength (kN/m)	49.91 ^b	49.5 ^c
Initial Young's Modulus E, MPa	120	52.3
Secant Modulus at 2.5% strain, MPa	60	47
Secant Modulus at 5 % strain, MPa	44	45

Note: MD = Machine direction; CD = Cross machine direction; E = Elastic modulus.

^aASTM D5261 (ASTM 2003a); ^bASTM D6637 (ASTM 2001);

^cASTM D4632 (ASTM 2003b)

was procured from Dhanaury village in Haridwar district, Uttarakhand state. The particle size distribution curves and typical characteristics of these materials are also given in Fig. 1 and Table 2, respectively.

3.3 Geogrid and Geotextile

A biaxial geogrid (GG) (Fig. 2c) and a non-woven geotextile (GT) (Fig. 2d) are used in the model tracks. The geotextile was a non-woven, heat-bonded, polypropylene (PP) fabric with an initial tensile stiffness of 115 kN/m and a thickness of 2.2 mm. The geogrid was made up of high density polyethylene (HDPE) with an aperture size of 30 mm x 30 mm and an initial tensile stiffness of 240 kN/m. Wide-width tensile tests were performed on the geogrid and geotextile on a tensile testing machine. The secant modulus is calculated from the stress-strain curve. The slope of a secant drawn from the origin to a particular point on the stress-strain curve is known as secant modulus. All the properties of geosynthetic materials are given in Table 3.

4. Testing equipment and procedure

Conventional triaxial apparatus was used for testing subgrade soil and subballast material, the size of sample being 38 mm diameter and 76 mm height. For subgrade soil, monotonic tests are performed under undrained conditions. For subballast material, slow consolidated drained tests were conducted. The ballast specimen tested was 380 mm in diameter and 813 mm in height. The shearing rate chosen was 0.5 % per minute. Consolidated drained tests with measurement of volume change were conducted on the ballast material.

A total of 5 tests were conducted in model test. Details of these tests are given in Table 4. The tests were termed as DC20 indicating that the models had Dhanaury clay (DC) as the subgrade soil and a subballast thickness (dsb) of 20 cm. In this test, one monotonic and four cyclic tests were conducted (Table 4).

The monotonic test (UR-M) and the first cyclic test (UR-C) were conducted on unreinforced model tracks; the second cyclic test (GT) was conducted on a model track stabilized with geotextile alone; the third cyclic test (GG) on a model track reinforced with geogrid alone; and the fourth cyclic test (GT-GG) on a model track reinforced with both geotextile and geogrid. The thicknesses of the ballast layer and the subgrade in all the models were kept constant equal to 116.7 mm and 500 mm, respectively. The photograph of a typical model test setup is shown in Fig. 3.

4.1 Interface tests

A typical railway track structure consists of several layers of different materials. The shear stiffness, normal

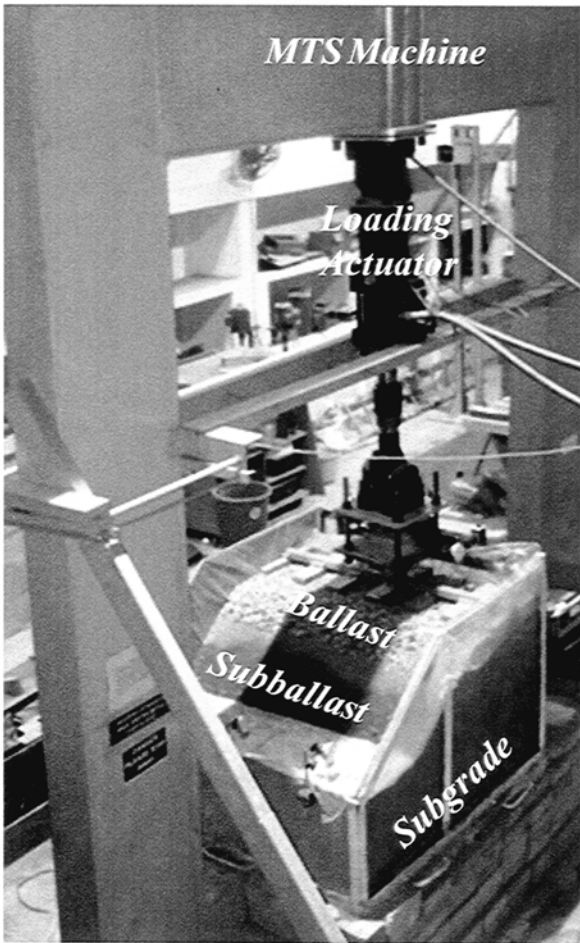


Fig. 3. Model test setup.

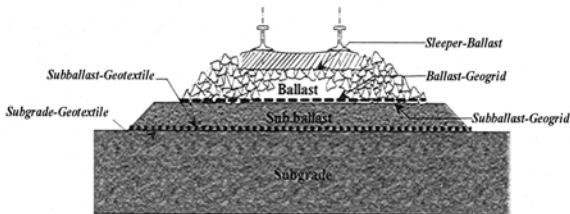


Fig. 4. Various interfaces in a railway track.

Table 4. Summary of model tests conducted on track.

Test type	Reinforcement Type	Loading Type
DC20 UR-M	No reinforcement	Monotonic
DC20 UR-C	No reinforcement	Cyclic
DC20 GT	Geotextile	Cyclic
DC20 GG	Geogrid	Cyclic
DC20 GG-GT	Geogrid and Geotextile	Cyclic

stiffness and interface friction angle between different materials are known to have influence on the strength-deformation behavior of the system. Interfaces provide displacement discontinuity between two different constituent materials. For geotechnical engineers,

interface friction that arises between various geomaterials is of great concern. This has particularly gained much significance with the application of the finite element method in geotechnical engineering.

Direct shear tests have been conducted to determine the interface properties including the normal stiffness, shear stiffness and interface friction angle between different track materials, namely, sleeper-ballast, ballast-geogrid, geogrid-subballast, subballast-geotextile and geotextile-subgrade (Fig. 4). The interface tests have been conducted in a small size direct shear apparatus with a box dimension of 60 mm x 60 mm x 50 mm for those interfaces that have constituent materials of the maximum particle size less than 10 mm. For the interfaces that have coarser constituent materials, a large size direct shear apparatus with a box dimension of 30 cm x 30 cm x 22.5 cm has been used.

5. Results and discussions

The results of CD triaxial tests in terms of deviator stress and volumetric strain versus axial strain on reduced size ballast samples termed here as ballast IA ($D_r = 87\%$) is shown in Fig. 5.

A nonlinear strain hardening deviator stress-strain relationship was observed for all samples. Deviator stress increased with increasing axial strain till failure, after which the deviator stress become almost constant. Volumetric compression was noted for all samples. As the confining stresses increased, the particle breakage also increased (Sowmiya, 2013).

The CD triaxial tests results for subballast sample is given in Fig. 6 in terms of variations of deviator stress with axial strain. As the axial strain increased, the deviator stress also increased nonlinearly. The deviator stress reached the peak at the axial strain ranging between 6-10 % depending upon the confining stresses and then decreased slightly thereafter.

The full saturation in CU tests was ensured by performing the consolidation stage under elevated value of backpressure (= 250 kPa) for 24 hours and then measuring B-value as 0.96 to 0.98. The test results in terms of deviator stress-strain relationship for Dhanaury clay is given in Fig. 7. A non-linear, strain hardening, stress-strain relationship was observed for the Dhanaury clay soil.

5.1 Model tests

5.1.1 Monotonic tests

First, a strain controlled monotonic test was conducted on an unreinforced track. The result of this test was then used to determine the magnitude of the

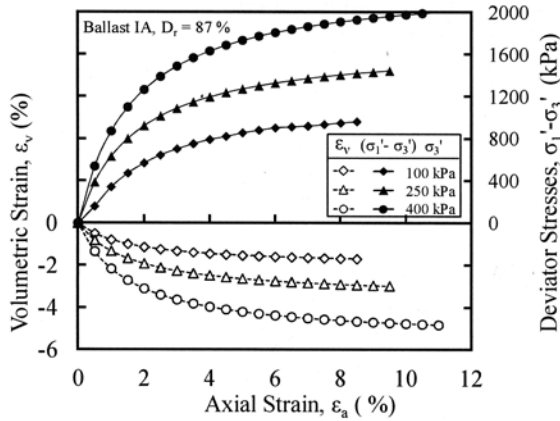


Fig. 5. Stress strain response of ballast sample.

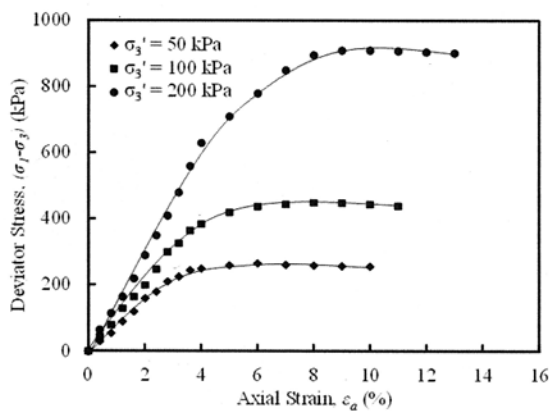


Fig. 6. Stress strain response of subballast sample.

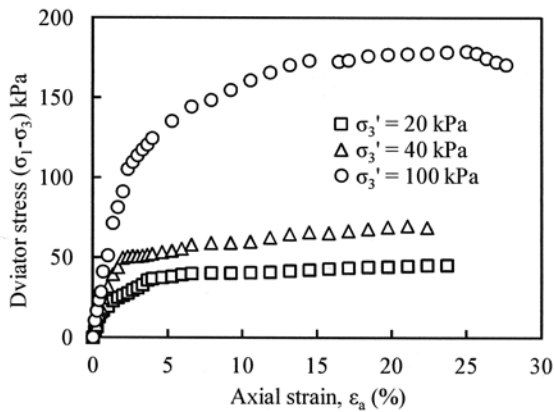


Fig. 7. Stress strain response of subgrade soil.

cyclic load to be applied during subsequent cyclic load tests in that group. During monotonic tests, the loading was carried out at a strain rate of 4 mm/min. The applied load versus track settlement (or the deflection of the loaded tie, δt) relationships for the monotonic test is plotted in Fig.8. As the applied load increases, the tie deflection also increases. A versatile ultimate load criterion defines the ultimate load as the point where the slope of the load-settlement curve first reaches zero or a

steady, minimum value (Vesic, 1963). Based on this, the failure load under monotonic loading for unreinforced track in DC20UR-M was obtained as 13.75 kN. Based on this, cyclic load of 9 kN (Threshold stress ratio, TSR = 65 %) was used for all cyclic tests under DC20 test group.

The model tracks with Dhanaury clay subgrade continued to exhibit stiff behavior until failure and the load-settlement curve resembled that of a general shear behavior (Vesic, 1963).

5.1.2 *Cyclic tests*

Figure 9 shows the relationship between the numbers of load cycles N versus the displacements of the loaded tie, δt for the model tests in DC20 test group. The figure shows that the presence of the geotextile at the subballast-subgrade interface (GT test) or the geogrid at the ballast-subballast interface (GG test) or both the geotextile and the geogrid at their respective interfaces (GT-GG test) reduces the tie displacement as compared to those for the corresponding unreinforced track (UR test). The maximum reduction in the tie displacement at the end of 25000 load cycles is observed in case of GT-GG test (42 %), followed by GG test (31 %) and GT test (19 %) as expected. The geogrid reinforcement is more effective owing to its nearness to the applied load and its higher stiffness as compared to the geotextile.

After the cyclic loading, post cyclic-monotonic loading was applied to determine the stiffness and failure load of the model track. Typical cyclic and post cyclic-monotonic responses for DC20 UR test are shown in Fig. 8.

At the end of the post cyclic-monotonic loading, the model tracks were dismantled layer-by-layer to observe the condition of the reinforcements (geogrid and geotextile). The geogrid had developed kinks in the rib at several places beside the wheel load along a continuous line in the direction perpendicular to the sleepers (Fig. 10a). During the post cyclic-monotonic loading, as the load increased, an increasingly higher confining stresses were mobilized in the ballast layer owing to the interlocking between the geogrid and ballast particles. Ultimately, geogrid ribs were twisted and developed kinks.

6. **Finite element analysis**

For the simulation of model tracks, first three-dimensional finite element models of exactly the same geometry as the laboratory model tracks were prepared. The materials of different track-layers were represented by the sets of constitutive relationships which are shown in Table 5.

6.1 Model tests

Hyperbolic Duncan Chang constitutive relationship is used as a non-linear model to simulate the ballast, subballast and subgrade soil. The input parameters K_L , n and K_b , m related to a non-linear variation of initial Young's modulus and Poisson's ratio, respectively, with confining stress were determined from triaxial tests. Rail and sleepers are modelled as elastic. Geogrid or/and geotextile are simulated using von Mises elastic-perfectly plastic relationship wherein input parameters are Elastic modulus E and yield stress σ_y which were determined from the wide width tensile test (ASTM, 2001). Coulomb friction model is used to simulate the interface elements.

7. Finite element simulation of model test tracks

All track components, namely, rail, sleeper, ballast and subballast layers, subgrade, geotextile and geogrid are modelled using 10-noded tetrahedral elements. Each component was meshed individually. The auto mesh option automatically generates meshes for the selected solids. Proper element size with adaptive seeding was applied. All the track components were separated with a "Boolean cut" operation before the mesh could be automatically generated.

7.1 Boundary conditions

Roller supports were used on the vertical faces of the track layers; however, no boundary conditions were applied on to the sloping faces of ballast and subballast layers, and to the sides of the rail. The bottom face of the subgrade was considered as fixed.

7.2 Comparison with model test results

Figure 8 compares the predicted results by the finite element analysis with the measured results during monotonic tests on unreinforced tracks (DC20 UR-M) in terms of load versus tie displacement. The FEM analysis gives a good prediction of the measured load-displacement relationship. The failure load under monotonic loading for unreinforced track in DC20 UR-M was obtained as 13.75 kN. The cyclic load of 9 kN (Threshold Stress Ratio, $TSR = \text{threshold stress}/\text{monotonic failure stress} = 65\%$), that were expected to induce slightly higher stresses on to the subgrade than the corresponding threshold stress of the subgrade soil in case of unreinforced track was used for all cyclic tests under DC20 group.

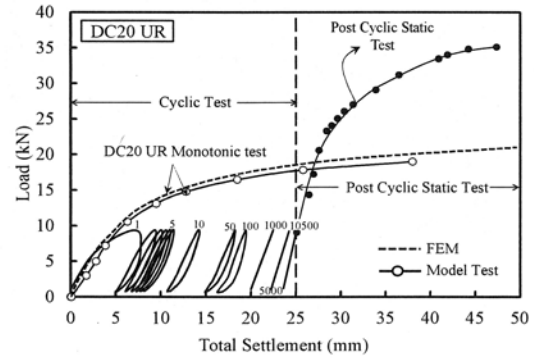


Fig. 8. Typical cyclic and post cyclic monotonic test responses of DC20 UR test.

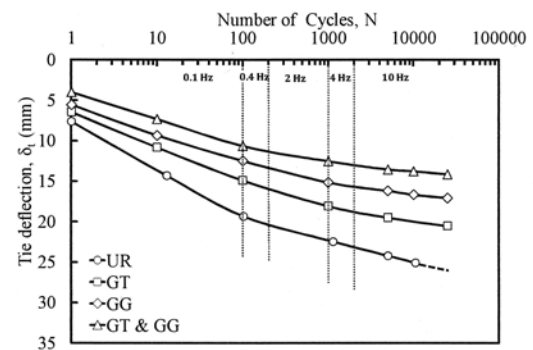


Fig. 9. Cyclic test responses of DC20 test group.

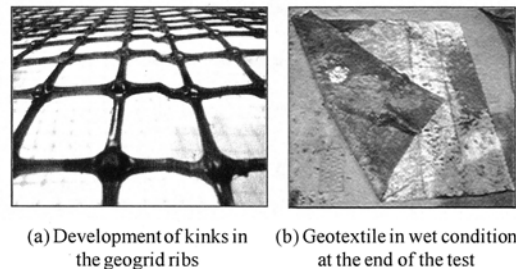


Fig. 10. Condition of reinforcements at the end of the post cyclic-monotonic loading.

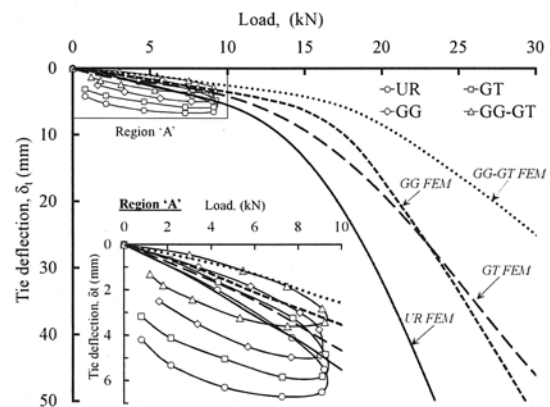


Fig. 11. Model test comparison with finite element analyses for DC20 test group (with Dhanaury clay as subgrade and subballast thickness of 200 mm).

Table 5. Summary of model tests conducted on track.

Track components	Non-linear analysis									
	Model used in Finite Element Analysis	E (MPa)	μ	c_u (kPa)	ϕ'	K_L	n	K_b	m	$\dagger\sigma_y$ (MPa)
Rail	Elastic	200000	0.27	-	-	-	-	-	-	-
Sleeper	Elastic	200000	0.27	-	-	-	-	-	-	-
Ballast	Duncan Chang	-	-	0.1	47.6°	477.9	0.575	508.6	0.136	-
Subballast	Duncan Chang	-	-	0.1	41.7°	97.7	0.414	108.7	0.046	-
Dhanaury clay	Duncan Chang	-	0.49	$\cong 8$	0.1	48.9	0.500	-	-	-
Geogrid	von Mises	120	0.20	-	-	-	-	-	-	14.4
Geotextile	von Mises	52.3	0.20	-	-	-	-	-	-	13.0

Note: \dagger Yield stress $\sigma_y = \frac{\sigma_1}{\sqrt{3}}$, and σ_1 = yield strength of geosynthetics in uniaxial direction.

The details of the cyclic test of DC20 group on unreinforced model track (DC20 UR-C) in terms of load with the tie displacement are shown in Fig. 9. Figure 11 shows the measured load versus tie displacement results during the first loading cycle up to 9 kN load for the cyclic tests of DC20 group with the predicted results by the FEM analysis. The measured results compare well with the predicted results up to 9 kN for all tests. Further, the complete load-tie displacement relationship up to failure has been predicted using the finite element analysis. All the four track sections (one unreinforced and three reinforced) exhibit a non-linear behavior and the curves resemble that of a typical general shear failure.

Typical vertical stress contours for the reinforced section DC20 GG-GT for the complete track as well as for individual layers are shown in Fig. 12. The stress contours of individual layers clearly show the distribution and dissipation of vertical stresses under the wheel loads. The stresses are highest in the ballast layer and decrease in the subsequent layers below in that order. Due to the presence of the reinforcement, the stresses are distributed to a much larger area; consequently, the vertical stresses under the wheel load decrease (Sowmiya et al., 2013).

Figure 13 compares the scatter of measured vertical stresses beneath the rail seat at the top of ballast (σ_b), subballast (σ_{sb}) and subgrade (σ_{sg}) during cyclic loading at approximately 9 kN load (i.e., at the peak of load cycles) with the predicted stresses by non-linear analyses for different model tests under DC20 group. In general, predicted vertical stresses lie roughly at the bottom of the measured scatter values. This may be because while the measured stresses were recorded during cyclic loading, the predictions were made for the static loading.

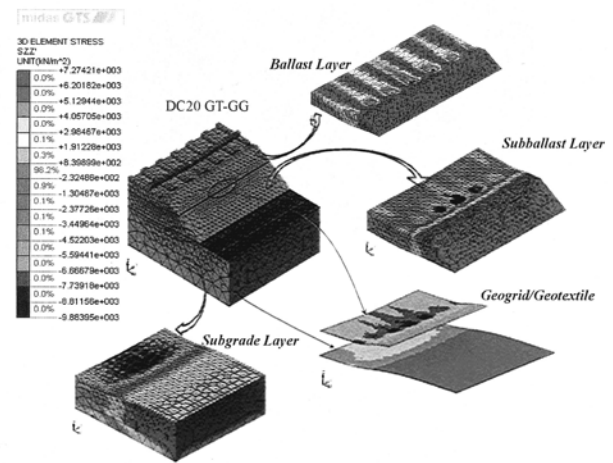


Fig. 12. Vertical stress contour for different components of DC20 GG-GT model.

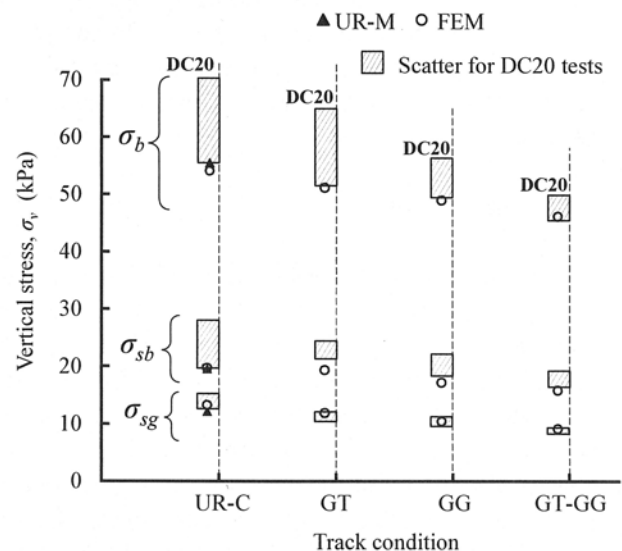


Fig. 13. Vertical stresses on top of each layers: comparison of model test results with FEM for DC20 test group.

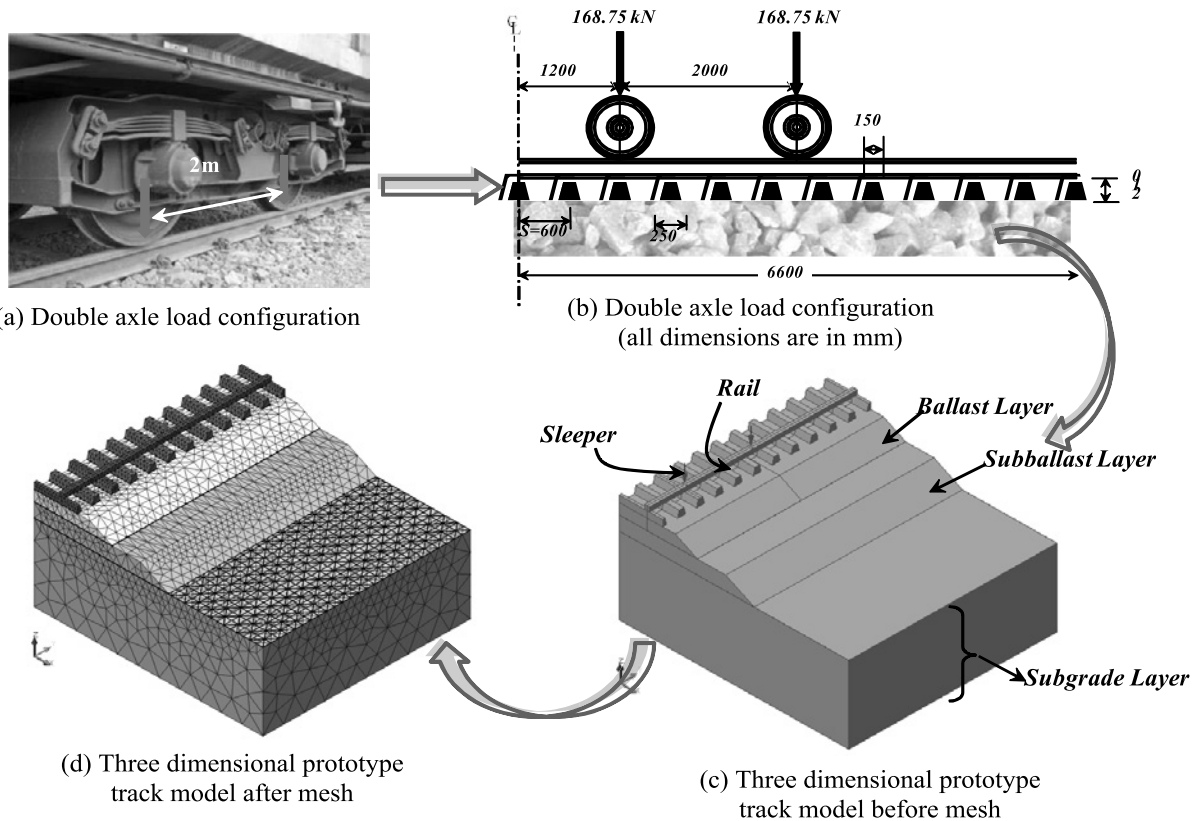


Fig. 14. Three dimensional finite element model of railway track with double axle load configuration.

8. Parametric study of prototype track

A detailed parametric study of a typical prototype track has been carried out to evaluate the effect of geosynthetics on track reinforcement using the FEM analysis. The parametric study has been carried out by first choosing a nominal track section and then varying different track parameters with reference to this nominal section.

8.1 Track sections

The nominal track section used for the parametric study is given in Fig. 14. Figure 14 shows the configuration of the train wheel load into a 3D finite element model and the subsequent finite element mesh. All other details of finite element simulation remain the same as used for the finite element analysis of the model tests. An axle load of 225 kN was considered with the impact factor of 1.5; thus the total axle load applied was 337.5 kN (or each wheel load = 168.75 kN). The details of the nominal track section are given in Tables 6 and 7.

Table 7 also gives the range in which a particular track parameter was varied while keeping all other track parameters at their nominal values. The parametric study has been carried out for both unreinforced and reinforced

track sections. A double wheel load configuration (inclusive of the impact factor 1.5) based on two adjacent car spacing was adopted as shown in the Fig. 14(b). Owing to symmetry, only one-fourth of the track section was modeled.

Table 6. Fixed track properties for parametric study.

Parameter	Nominal Value
Poisson's Ratio	
Rail, μ_r	0.27
Tie or Sleeper, μ_t	0.2
Ballast, μ_b	0.35
Sub-ballast, μ_{sb}	0.32
Subgrade, μ_{sg}	0.3
Rail Modulus, E_r	200×10^3 MPa
Distance of rail from center line of tie	0.875 m
Tie	
Thickness, t_t	0.21 m
Width, B_t (bottom and top)	0.25 m and 0.15 m
Length, L_t	2.75 m
Spacing, S	0.6 m
Modulus, E_t	30×10^3 MPa
Geogrid	
Thickness, t_{gg}	5 mm
Geotextile	
Thickness, t_{gt}	3.5 mm
Subgrade thickness, d_{sg}	2.5 m
Wheel load, Q (double axle)	168.75 kN/wheel

8.2 Parametric variations

8.2.1 Effect of subgrade stiffness (E_{sg}) and subballast thickness (d_{sb})

Figure 15 shows the effect of the subgrade stiffness (E_{sg}) on the tie displacement of the unreinforced and reinforced sections. In view of the reinforcement function of the geogrid, a single (at ballast-subballast interface) and two layers (one each at ballast subballast and subballast-subgrade interfaces) of geogrid reinforcement have been considered for the analysis. Three different Young's moduli of subgrade (1.5, 5 and 15 MPa) with a nominal subballast thickness of 450 mm were used for the analysis.

The load displacement curves show that at any given load, as the stiffness of the subgrade increases, the tie displacement decreases (Fig. 15).

Figure 16 shows that the tie displacements δ_{max} of the track with $d_{sb} = 300$ mm and 450 mm reinforced with two geogrid layers was lower than the unreinforced track with $d_{sb} = 1000$ mm. Thus, the inclusion of two geogrid layers at proper interfaces can reduce the consumption of subballast materials by approximately 55-70 %. This is especially economical and useful where the subballast material is procured from long haul distances.

9. Conclusions

The results of monotonic and cyclic tests on reinforced track models are presented to evaluate the influence of type of geosynthetic reinforcement, subballast thickness and type of subgrade on displacements and induced vertical stresses on each track layer. Based on the model test and the finite element analyses results, the following conclusions are drawn.

In case of Dhanaury clay subgrade, the model tracks reinforced with only geogrid (GG track) at ballast-subballast interface are more effective in reducing the tie displacements, ballast and subballast strains, and subgrade displacements as compared to the model tracks reinforced with only geotextile (GT track) at subballast-subgrade interface. The geogrid is more effective owing to its nearness to the applied load and higher stiffness as compared to the geotextile. The measured stresses and displacements in the model tests were compared with the results predicted using the FEM analysis. The comparison shows that FEM analysis is able to predict the measured results accurately. Based on this, further the analysis was extended to the field by performing finite element analysis of prototype track.

Table 7. Fixed track properties for parametric study.

Parameter	Nominal Value	Range
Modulus of Elasticity (MPa)		
Geogrid, E_{gg}	1000	120, 2000, 4000
Geotextile, E_{gt}	100	-
Modulus of subgrade, E_{sg} (MPa)		
Sub-ballast layer thickness, d_{sb} (m)	0.45	0.3, 0.6, 1

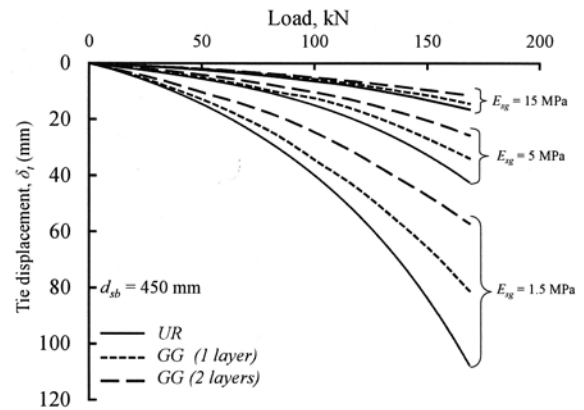


Fig. 15. Effect of Young's modulus of subgrade (E_{sg}) on tie displacement for prototype tracks.

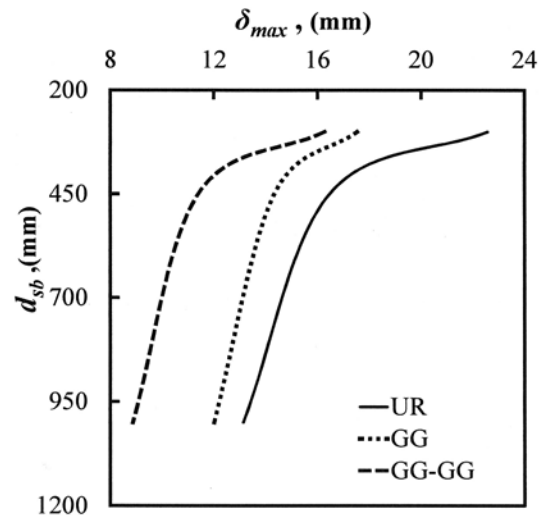


Fig. 16. Model test comparison with finite element analyses for DC20 test group (with Dhanaury clay as subgrade and subballast thickness of 200 mm).

As the subgrade stiffness increases, induced vertical stresses and displacements at the top of each layer in a reinforced section as well as an unreinforced section decrease owing to a better stress distribution. The benefit

of the reinforcement in terms of percentage reduction in stresses and displacements is higher when the subgrade soil is soft. Geogrids with higher stiffness reduce the tie displacements better than the geogrids with lower stiffness.

References

- ASTM, 2001. Standard test method for determining tensile properties of geogrids by the single or multi-rib tensile method. D6637, West Conshohocken, PA.
- ASTM, 2003a. Standard test method for measuring mass per unit area of geotextiles. D5261, West Conshohocken, PA.
- ASTM. 2003b. Standard test method for grab breaking load and elongation of geotextiles. D4632, West Conshohocken, PA.
- Brown, S.F., Kwan, J. and Thom, N.H., 2007. Identifying the key parameters that influence geogrid reinforcement of railway ballast. *Geotextiles and Geomembranes*, **25**: 326-335.
- Indraratna, B., Khabbaz, H., Salim, W. and Christie, D., 2006. Geotechnical properties of ballast and the role of geosynthetics in railway track stabilization. *Ground Improvement*, **10** (3): 91-101.
- Midas GTS manual, 2013. Geotechnical and tunnel analysis system reference manual for modeling, integrated design and analysis.
- ORE, 1982. The behaviour of the track bed structure under repeated loading (First phase-Vienna Arsenal Tests), In Question D117-Optimum adoption of the conventional track to future traffic. Office for Research and Experiments, Intl. Union of Railways, Utrecht, The Netherlands, Report D117/RP18.
- ORE, 1983. The behaviour of the track bed structure under repeated loading (Tests at Vienna Arsenal and Derby), In Question D117-Optimum adoption of the conventional track to future traffic. Office for Research and Experiments, Intl. Union of Railways, Utrecht, The Netherlands, Report D117/RP25.
- Raymond, G.P., 2002. Reinforced ballast behaviour subjected to repeated load. *Geotextiles and Geomembranes*, **20**: 39-61.
- Raymond, G.P., and Davies, J.R., 1978. Triaxial tests on dolomite railroad ballast. *J. Geotech. Engrg. Div., ASCE*, **104** (6): 737-751.
- Selig. E.T., 1991. Field trip to Conrail Site at Pottstown, PA (U.S.A), June 5, 1990. Trip Report, April.
- Shahu, J.T., Kameswara Rao, N.S.V. and Yudhbir., 1999. Parametric study of resilient response of tracks with a subballast layer. *Can. Geotech. Journal*, **36**: 1137-1150.
- Shahu, J.T., Yudhbir., and Kameswara Rao, N.S.V., 2000. A rational method for design of railroad track foundation. *Soils and Foundations*, **40** (6): 1-10.
- Shin, E.C., Kim, D.H. and Das, B.M., 2002. Geogrid-reinforced railroad bed settlement due to cyclic load. *J. Geotech. and Geol. Engrg., Springer Netherlands*, **20** (3): 261-271.
- Sowmiya, L.S., 2013. Analysis and experimental investigations of railway tracks with and without geosynthetic reinforcement. Ph.D. Thesis, Indian Institute of Technology, Delhi, India (unpublished).
- Sowmiya, L.S., Shahu, J.T. and Gupta, K.K., 2013. Stresses and displacements in reinforced tracks. *Ground Improvement*, **167** (1): 47-59.
- Vesic, A.S., 1963. Bearing capacity of deep foundations in sands. National Academy of Science, National Research Council, Highway Research Record, **39**:112-153.